Observation of $D_{s1}(2536)^+ \to D^+\pi^-K^+$ and angular decomposition of $D_{s1}(2536)^+ \to D^{*+}K^0_S$

V. Balagura,[14] I. Adachi,[9] H. Aihara,[44] K. Arinstein,[1] V. Aulchenko,[1] T. Aushev,[19,14] A. M. Bakich,[40] E. Barberio,[22] A. Bay,[19] K. Belous,[13] V. Bhardwaj,[34] U. Bitenc,[15] A. Bondar,[1] A. Bozek,[28] M. Bračko,[15,21] J. Brodzicka,[9] T. E. Browder,[8] M.-C. Chang,[4] Y. Chao,[27] A. Chen,[25] W. T. Chen,[25] B. G. Cheon,[7] R. Chistov,[14] I.-S. Cho,[49] Y. Choi,[39] J. Dalseno,[22] M. Danilov,[14] A. Drutskoy,[3] S. Eidelman,[1] D. Epifanov,[1] N. Gabyshev,[1] A. Garmash,[35] B. Golob,[15,20] H. Ha,[17] J. Haba,[9] T. Hara,[33] N. C. Hastings,[44] K. Hayasaka,[23] H. Hayashii,[24] M. Hazumi,[9] D. Heffernan,[33] Y. Hoshi,[42] W.-S. Hou,[27] H. J. Hyun,[18] K. Inami,[23] A. Ishikawa,[36] H. Ishino,[45] R. Itoh,[9] M. Iwasaki,[44] Y. Iwasaki,[9] D. H. Kah,[18] H. Kaji,[23] N. Katayama,[9] H. Kawai,[2] T. Kawasaki,[30] H. Kichimi,[9] H. J. Kim,[18] H. O. Kim,[39] Y. J. Kim,[6] K. Kinoshita,[3] S. Korpar,[15,21] P. Križan,[15,20] P. Krokovny,[9] C. C. Kuo,[25] A. Kuzmin,[1] Y.-J. Kwon,[49] J. S. Lange,[5] M. J. Lee,[38] S. E. Lee,[38] T. Lesiak,[28] A. Limosani,[22] S.-W. Lin,[27] Y. Liu,[6] D. Liventsev,[14] F. Mandl,[12] S. McOnie,[40] T. Medvedeva,[14] W. Mitaroff,[12] H. Miyake,[33] H. Miyata,[30] Y. Miyazaki,[23] R. Mizuk,[14] D. Mohapatra,[48] G. R. Moloney,[22] Y. Nagasaka,[10] E. Nakano,[32] M. Nakao,[9] H. Nakazawa,[25] Z. Natkaniec,[28] S. Nishida,[9] O. Nitoh,[47] S. Ogawa,[41] T. Ohshima,[23] S. Okuno,[16] S. L. Olsen,[8,11] W. Ostrowicz,[28] H. Ozaki,[9] P. Pakhlov,[14] G. Pakhlova,[14] H. Palka,[28] C. W. Park,[39] L. S. Peak,[40] R. Pestotnik,[15] L. E. Piilonen,[48] Y. Sakai,[9] O. Schneider,[19] K. Senyo,[23] M. Shapkin,[13] C. P. Shen,[11] H. Shibuya,[41] J.-G. Shiu,[27] A. Somov,[3] S. Stanič,[31] M. Starič,[15] T. Sumiyoshi,[46] K. Tamai,[9] M. Tanaka,[9] G. N. Taylor,[22] Y. Teramoto,[32] I. Tikhomirov,[14] S. Uehara,[9] K. Ueno,[27] T. Uglov,[14] Y. Unno,[7] S. Uno,[9] P. Urquijo,[22] Y. Usov,[1] G. Varner,[8] K. Vervink,[19] S. Villa,[19] A. Vinokurova,[1] C. C. Wang,[27] C. H. Wang,[26] M.-Z. Wang,[27] P. Wang,[11] X. L. Wang,[11] Y. Watanabe,[16] E. Won,[17] B. D. Yabsley,[40] A. Yamaguchi,[43] Y. Yamashita,[29] M. Yamauchi,[9] Z. P. Zhang,[37] V. Zhilich,[1] V. Zhulanov,[1] A. Zupanc,[15] and O. Zyukova[1]

(The Belle Collaboration)

[1]*Budker Institute of Nuclear Physics, Novosibirsk*
[2]*Chiba University, Chiba*
[3]*University of Cincinnati, Cincinnati, Ohio 45221*
[4]*Department of Physics, Fu Jen Catholic University, Taipei*
[5]*Justus-Liebig-Universität Gießen, Gießen*
[6]*The Graduate University for Advanced Studies, Hayama*
[7]*Hanyang University, Seoul*
[8]*University of Hawaii, Honolulu, Hawaii 96822*
[9]*High Energy Accelerator Research Organization (KEK), Tsukuba*
[10]*Hiroshima Institute of Technology, Hiroshima*
[11]*Institute of High Energy Physics, Chinese Academy of Sciences, Beijing*
[12]*Institute of High Energy Physics, Vienna*
[13]*Institute of High Energy Physics, Protvino*
[14]*Institute for Theoretical and Experimental Physics, Moscow*
[15]*J. Stefan Institute, Ljubljana*
[16]*Kanagawa University, Yokohama*
[17]*Korea University, Seoul*
[18]*Kyungpook National University, Taegu*
[19]*École Polytechnique Fédérale de Lausanne (EPFL), Lausanne*
[20]*University of Ljubljana, Ljubljana*
[21]*University of Maribor, Maribor*
[22]*University of Melbourne, School of Physics, Victoria 3010*
[23]*Nagoya University, Nagoya*
[24]*Nara Women's University, Nara*
[25]*National Central University, Chung-li*
[26]*National United University, Miao Li*
[27]*Department of Physics, National Taiwan University, Taipei*
[28]*H. Niewodniczanski Institute of Nuclear Physics, Krakow*
[29]*Nippon Dental University, Niigata*
[30]*Niigata University, Niigata*
[31]*University of Nova Gorica, Nova Gorica*
[32]*Osaka City University, Osaka*
[33]*Osaka University, Osaka*
[34]*Panjab University, Chandigarh*

[35]*Princeton University, Princeton, New Jersey 08544*
[36]*Saga University, Saga*
[37]*University of Science and Technology of China, Hefei*
[38]*Seoul National University, Seoul*
[39]*Sungkyunkwan University, Suwon*
[40]*University of Sydney, Sydney, New South Wales*
[41]*Toho University, Funabashi*
[42]*Tohoku Gakuin University, Tagajo*
[43]*Tohoku University, Sendai*
[44]*Department of Physics, University of Tokyo, Tokyo*
[45]*Tokyo Institute of Technology, Tokyo*
[46]*Tokyo Metropolitan University, Tokyo*
[47]*Tokyo University of Agriculture and Technology, Tokyo*
[48]*Virginia Polytechnic Institute and State University, Blacksburg, Virginia 24061*
[49]*Yonsei University, Seoul*

(Received 26 September 2007; published 14 February 2008)

Using 462 fb^{-1} of e^+e^- annihilation data recorded by the Belle detector, we report the first observation of the decay $D_{s1}(2536)^+ \to D^+\pi^-K^+$. The ratio of branching fractions $\frac{\mathcal{B}(D_{s1}(2536)^+\to D^+\pi^-K^+)}{\mathcal{B}(D_{s1}(2536)^+\to D^{*+}K^0)}$ is measured to be $(3.27 \pm 0.18 \pm 0.37)\%$. We also study the angular distributions in the $D_{s1}(2536)^+ \to D^{*+}K^0_S$ decay and measure the ratio of D- and S-wave amplitudes. The S-wave dominates, with a partial width of $\Gamma_S/\Gamma_{\text{total}} = 0.72 \pm 0.05 \pm 0.01$.

DOI: 10.1103/PhysRevD.77.032001 PACS numbers: 13.25.Ft, 11.80.Et, 13.66.Bc, 13.88.+e

I. INTRODUCTION

Two states, $D^*_{s0}(2317)^+$ and $D_{s1}(2460)^+$, have been discovered recently both in continuum e^+e^- annihilation near $\sqrt{s} = 10.6$ GeV/c^2 and in B meson decays [1–3]. Their spin parities are, respectively, $J^P = 0^+$ and 1^+ [4], and they are presumed to be P-wave excited $c\bar{s}$ states with $j = |\vec{L} + \vec{S}_{\bar{s}}| = 1/2$. Here, $|\vec{L}| = 1$ is the orbital angular momentum and $\vec{S}_{\bar{s}}$ is the spin of the light antiquark. However, their masses are unexpectedly low [5]. This has renewed interest in measurements of P-wave excited charm mesons such as $D_{s1}(2536)^+$ and $D_{s1}(2460)^+$.

We report the first observation of the decay $D_{s1}(2536)^+ \to D^+\pi^-K^+$. (The inclusion of charge-conjugate modes is implied throughout this paper.) The $D^+\pi^-$ pair in the final state is the only $D\pi$ combination that cannot come from a D^* resonance: D^{*0} mesons can only be produced virtually here since $M_{D^{*0}} < M_{D^+} + M_{\pi^-}$. The new $D_{s1}(2536)^+ \to D^+\pi^-K^+$ mode reported here is only the second observed three-body decay of the $D_{s1}(2536)^+$, after $D^+_s\pi^+\pi^-$ [3,6].

In addition, we have performed an angular analysis of the $D_{s1}(2536)^+ \to D^{*+}K^0_S$ mode. Heavy quark effective theory (HQET) predicts that for an infinitely heavy c-quark this decay of a $J^P = 1^+$, $j = 3/2$ state should proceed via a pure D-wave [7]. The corresponding decay of its partner, the $D_{s1}(2460)^+$, which is believed to be a 1^+, $j = 1/2$ state is energetically forbidden, but if it were allowed it would proceed via a pure S-wave. Since heavy quark symmetry is not exact, the two 1^+ states can mix with each other,

$$\begin{aligned} |D_{s1}(2460)^+\rangle &= \cos\theta|^{1/2}E_1\rangle + \sin\theta|^{3/2}E_1\rangle, \\ |D_{s1}(2536)^+\rangle &= -\sin\theta|^{1/2}E_1\rangle + \cos\theta|^{3/2}E_1\rangle, \end{aligned} \quad (1)$$

where $|^{1/2}E_1\rangle$ and $|^{3/2}E_1\rangle$ denote the states with $j = 1/2$ and $j = 3/2$, respectively. Note that the coupling via common decay channels can give a contribution to the mixing that might not be well represented by an orthogonal rotation [8]. We neglect this possibility in the expression above. If $\theta \neq 0$, an S-wave component can appear in the decay $D_{s1}(2536)^+ \to D^*K$. Moreover, even if θ is small, the S-wave component can give a sizeable contribution to the width because the D-wave contribution is strongly suppressed by the small energy release in the $D_{s1}(2536)^+ \to D^*K$ decay.

The first attempt to decompose S- and D-waves in the analogous decays of the nonstrange mesons $D_1(2420)^0 \to D^{*+}\pi^-$ and $D_1(2420)^+ \to D^{*0}\pi^+$ was reported more than ten years ago by CLEO [9,10]; currently, no results on the $D_{s1}(2536)^+$ exist. Moreover, CLEO's method did not allow the measurement of the ratio of partial widths: it only determined the relation between this ratio and the relative phase between the S- and D-wave amplitudes. Some information on θ is obtained from the ratio of electromagnetic decay rates $D_{s1}(2460)^+ \to D^+_s\gamma, D^{*+}_s\gamma$, since only the $^1P_1$ state in $D_{s1}(2460)^+$ undergoes an electric dipole ($E1$) transition to D^+_s and only the $^3P_1$ state to D^{*+}_s [11]. The bases $|^jE_1\rangle$ and $|^{2S+1}P_1\rangle$ are related by the rotation angle θ_0, where $\tan\theta_0 = -\sqrt{2}$. The angle between the bases $|D^+_s\rangle$ and $|^{2S+1}P_1\rangle$ is $\theta + \theta_0$. The Belle Collaboration studied $D_{s1}(2460)^+ \to D^+_s\gamma$, $D^{*+}_s\gamma$ decays using $D_{s1}(2460)^+$ from both B decays [2] and from e^+e^- annihilation [3], and determined the ratio of decay rates to be 0.4 ± 0.3 and 0.28 ± 0.17, respectively. The average ratio of 0.31 ± 0.14 gives the constraint $\tan^2(\theta + \theta_0) = 0.8 \pm 0.4$ using the formulas of Ref. [11]. Detailed knowledge of the mixing is important to test different theoretical

models [8,11,12], to fix their parameters, and to understand better the nature of D_{sJ} mesons.

Finally, using the $D_{s1}(2536)^+ \to D^{*+}K_S^0$ mode, we have measured the spin alignment of high momentum $D_{s1}(2536)^+$ mesons produced in e^+e^- annihilation. Production of excited mesons in the HQET framework is described in Ref. [13]. The fragmentation process is assumed to be so rapid that the color magnetic forces do not have time to act and thus the spin of the light antiquark in the produced meson is uncorrelated with that of the heavy quark. One consequence of this is that D^* mesons with $j = \frac{1}{2}$ are produced unpolarized. This was confirmed with good accuracy by CLEO [14] in $e^+e^- \to c\bar{c}$ events at $\sqrt{s} = 10.5$ GeV and was also checked by other experiments [15]. Another prediction is that D^* and D mesons are produced according to the number of available helicity states in a 3:1 ratio. However, experimental data from several different production mechanisms (e^+e^-, hadroproduction, photoproduction, etc.) give an average probability for an S-wave meson to be produced in a vector state of 0.594 ± 0.010 [16], which is much smaller than the expected value of 0.75.

There are no similar measurements for the P-wave states. Contrary to the S-wave mesons (D, D^*) case, HQET predicts that the members of the $j = 3/2$ doublet can be produced aligned. The probabilities for the light degree of freedom to have helicity $-3/2$, $-1/2$, $1/2$, $3/2$ are expressed via single, Falk-Peskin parameter $w_{3/2}$ as $\frac{1}{2}w_{3/2}$, $\frac{1}{2}(1 - w_{3/2})$, $\frac{1}{2}(1 - w_{3/2})$, $\frac{1}{2}w_{3/2}$, respectively. By adding the c-quark spin and resolving the $c\bar{s}$ system into 1^+ and 2^+ states, one can calculate their alignments. For $D_{s1}(2536)^+$ the probability of zero helicity is $\rho_{00} = \frac{2}{3} \times (1 - w_{3/2})$. A calculation based on perturbative QCD and a nonrelativistic quark model gives $w_{3/2} \approx 0.254$ [17]. This calculation also predicts the dependence of $w_{3/2}$ on the longitudinal momentum fraction and on the transverse momentum of the meson relative to the heavy quark jet. The ARGUS analysis of the angular distributions in $D_2^*(2460) \to D\pi$ decay [18] gives an upper limit $w_{3/2} < 0.24$ at 90% C.L. [13]. Once $w_{3/2}$ is measured, one can make definite predictions for the angular distributions of the remaining $j = 3/2$ meson decays and check the validity of HQET.

II. SELECTION CRITERIA

This study is based on a data sample of 462 fb^{-1} collected near the $\Upsilon(4S)$ resonance with the Belle detector at the KEKB asymmetric-energy e^+e^- (3.5 on 8 GeV) collider [19]. The Belle detector is a large-solid-angle magnetic spectrometer that consists of a silicon vertex detector, a 50-layer central drift chamber, an array of aerogel threshold Cherenkov counters, a barrel-like arrangement of time-of-flight scintillation counters, and an electromagnetic calorimeter comprised of CsI(Tl) crystals located inside a superconducting solenoid coil that provides a 1.5 T magnetic field. An iron flux-return located outside the coil is instrumented to detect K_L^0 mesons and to identify muons. The detector is described in detail elsewhere [20]. Two inner detector configurations were used. A 2.0 cm beampipe and a 3-layer silicon vertex detector were used for the first sample of 155 fb^{-1}, while a 1.5 cm beampipe, a 4-layer silicon detector, and a small-cell inner drift chamber were used to record the remaining 307 fb^{-1} [21].

$K^\pm$ and $\pi^\pm$ candidates are required to originate from the vicinity of the event-dependent interaction point. To identify kaons, we combine the ionization energy loss (dE/dx) from the central drift chamber, time of flight, and Cherenkov light yield information for each track to form kaon and pion likelihoods $\mathcal{L}_K$ and $\mathcal{L}_\pi$, respectively [22], and then impose the requirement $\mathcal{L}_K/(\mathcal{L}_K + \mathcal{L}_\pi) > 0.1$. This requirement has 98% (97%) efficiency for a kaon from $D_{s1}(2536)^+$ (kaon from D) and a 12% (17%) misidentification probability for a pion. All unused tracks, whether identified as a kaon or not, are treated as pion candidates in what follows. K_S^0 candidates are reconstructed via the $\pi^+\pi^-$ decay channel, requiring the two pions to originate from the common vertex and with a mass within ± 30 MeV/c^2 of the nominal K_S^0 mass. D^0 and D^+ mesons are reconstructed using $K^-\pi^+$, $K_S^0\pi^+\pi^-$, $K^-\pi^+\pi^+\pi^-$ and $K_S^0\pi^+$, $K^-\pi^+\pi^+$ decay modes, respectively. All combinations with masses within ± 20 MeV/c^2 of the nominal D mass are selected (99% efficiency); a mass and vertex constrained fit is then applied.

D^{*+} mesons are reconstructed using the $D^0\pi^+$ mode. The π^+ momentum in this reaction is low, typically between 100 MeV/c and 450 MeV/c in the laboratory frame for the selected candidates. The slow π^+ momentum resolution is degraded by multiple scattering, but is improved by a track refit procedure in which the π^+ origin point is constrained by the intersection of the D^0 momentum and the known e^+e^- interaction region. The $D^0\pi^+$ mass is required to be within ± 1.5 MeV/c^2 of the D^{*+} nominal value, which corresponds to 98% efficiency. A D^{*+} mass constraint is not imposed. Instead, we characterize the $D_{s1}(2536)^+$ candidate using the mass difference $M_{D^0\pi^+K_S^0} - M_{D^0\pi^+}$, where the error in the D^{*+} momentum nearly cancels out. For the $D_{s1}(2536)^+ \to D^+\pi^-K^+$ decay mode, the track refit procedure described above is applied to the pion and kaon momenta, and the $D_{s1}(2536)^+$ is characterized by the $D^+\pi^-K^+$ mass.

It is known that the momentum spectrum of the excited charm resonances from continuum e^+e^- annihilation is hard. In addition, due to the strong magnetic field in the Belle detector, the tracking efficiency for low momentum $\pi^\pm$ and K^+ mesons from D^{*+} and $D_{s1}(2536)^+$ decays rises with $D_{s1}(2536)^+$ momentum. Therefore, we require $x_P > 0.8$ for the scaled momentum x_P, defined as the ratio $p^*/p^*_{\rm max}$. Here, p^* is the momentum of the $D_{s1}(2536)^+$ candidate in the e^+e^- center-of-mass frame,

while $p^*_{\rm max} = \sqrt{E^{*2}_{\rm beam} - M^2_{D^+_{s1}}}$ is the momentum in this frame for a candidate carrying all the beam energy. This selection also removes $D_{s1}(2536)^+$ mesons produced in the decays of B mesons.

In Monte Carlo (MC) simulation, $D_{s1}(2536)^+$ mesons from e^+e^- annihilation, particle decays, and the detailed detector response are simulated using the PYTHIA, EvtGen, and GEANT packages [23–25], respectively. The D^0 and D^+ decay modes used in reconstruction are generated with their resonant substructures taken from the Particle Data Group (PDG) compilation [4] but neglecting any interference effects. The $D_{s1}(2536)^+$ momentum spectrum as measured with the $D_{s1}(2536)^+ \to D^{*+}K^0_S$ decay mode is used for MC generation. As shown below in Fig. 3, no clear resonant substructure is visible in the decay $D_{s1}(2536)^+ \to D^+\pi^-K^+$. Therefore, this mode is simulated as a three-body phase space decay. $D_{s1}(2536)^+ \to D^{*+}K^0_S$ decays are generated according to the results of the presented measurement of $D_{s1}(2536)^+$ polarization and D/S-wave interference [26].

III. $D_{s1}(2536)^+ \to D^+\pi^-K^+$ DECAY

The mass $M_{D^+\pi^-K^+}$ (upper plot) and the mass difference $(M_{D^0\pi^+K^0_S} - M_{D^0\pi^+}) + M^{\rm PDG}_{D^{*+}}$ (lower plot) for all accepted combinations are shown in Fig. 1. The PDG superscript denotes the nominal mass value from Ref. [4]. A clear peak for the new decay channel $D_{s1}(2536)^+ \to D^+\pi^-K^+$ is visible. The mass spectrum of the wrong sign combinations $D^+\pi^+K^-$ shown by the hatched histogram has no enhancement in the $D_{s1}(2536)^+$ region.

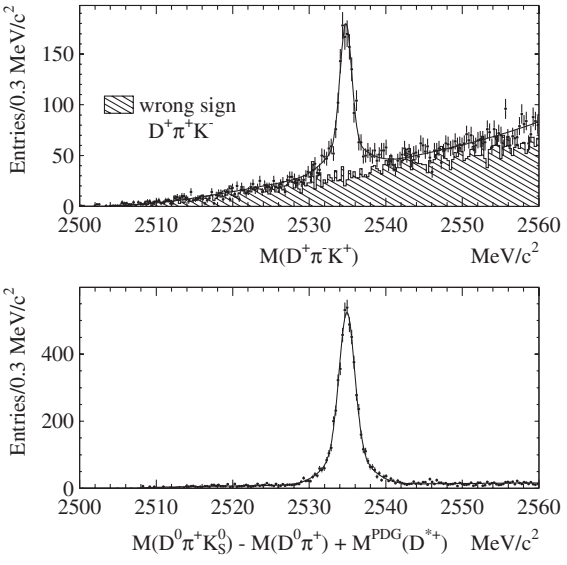

FIG. 1. Observed invariant mass spectra of selected $D^+\pi^-K^+$ (top) and $D^{*+}K^0_S$ (bottom) combinations. The hatched histogram in the top plot shows the corresponding spectrum of wrong sign $D^+\pi^+K^-$ combinations. The fit is described in the text. The fit results are listed in Table I.

To obtain the number of $D_{s1}(2536)^+$ decays, each of the distributions in Fig. 1 is fit to the sum of two Gaussians with a common mean (but not common between the two decay modes). To ensure that the second Gaussian is always wider than the first one, its width is chosen to be of the form $\sigma_2 = \sqrt{\sigma_1^2 + \Delta\sigma^2}$. The position of the peak, σ_1, $\Delta\sigma$, the fraction of events in the first Gaussian, and the total number of events in two Gaussians are allowed to vary in the fit. The background for the three-body $D^+\pi^-K^+$ (two-body $D^{*+}K^0_S$) mode is parametrized by a second (first) order polynomial multiplied by the threshold function $(M - M^{\rm thr}_{D^+\pi^-K^+})^2$ $(\sqrt{M - M^{\rm thr}_{D^{*+}K^0_S}})$, where $M^{\rm thr}_f$ is the sum of the nominal masses of final state particles f [4]. Table I contains the fit results together with the parameters of the Gaussians obtained from MC simulation. The MC efficiency is calculated as the weighted average for different D decay modes. Branching fractions of D^+, D^0 mesons as well as $\mathcal{B}(K^0_S \to \pi^+\pi^-)$, $\mathcal{B}(K^0 \to K^0_S)$, and $\mathcal{B}(D^{*+} \to D^0\pi^+)$ for the last row of Table I are taken from Ref. [4].

In the analysis we do not select the best $D_{s1}(2536)^+$ candidate in the event. If we did so, we would introduce an efficiency dependence on the presence and the distribution of random $D_{s1}(2536)^+$ candidates which is difficult to estimate reliably in MC. The small fraction of events contributing two entries to the $D_{s1}(2536)^+$ signal region in the mass plot is determined from data. Since the fraction can be different for the signal and background events, we use sideband subtraction procedure. The excess of double counted events in the signal region ($N^{\rm sig}_{\rm double}$) in comparison with the same number averaged over the left and the right sideband ($N^{\rm side}_{\rm double}$) is $N^{\rm sig}_{\rm double} - N^{\rm side}_{\rm double} = 35 - 18.5 = 16.5$ and $203 - 15.5 = 187.5$ for the $D^+\pi^-K^+$ and $D^{*+}K^0_S$ modes, respectively. These numbers are subtracted from the fitted yields and the results are presented in Table I. The same procedure is used in calculating the MC efficiency. The signal and the sidebands are defined as $|\Delta M_{D^+_{s1}}| < 5$ MeV/c^2, 10 MeV/$c^2 < |\Delta M_{D^+_{s1}}| < 20$ MeV/c^2, respectively, where $\Delta M_{D^+_{s1}}$ is measured relative to the peak position obtained from the fit.

The ratio of branching fractions is found to be

$$\frac{\mathcal{B}(D_{s1}(2536)^+ \to D^+\pi^-K^+)}{\mathcal{B}(D_{s1}(2536)^+ \to D^{*+}K^0)} = (3.27 \pm 0.18 \pm 0.37)\%, \quad (2)$$

where the first error is statistical and the second is systematic.

The systematic error receives contribution from the sources listed in Table II. A possible difference between the data and MC simulation in evaluation of the tracking efficiency is estimated using partially reconstructed D^{*+} decays. The reconstruction efficiency errors for low momentum K^+, K^0_S, and $\pi^\pm$ mesons from D^{*+} and $D_{s1}(2536)^+$ decays are added linearly since the tracking

TABLE I. Fit results for the $D_{s1}(2536)^+$ spectra in Fig. 1 and for the corresponding MC simulation spectra: the number of events in the two Gaussians for data *or the efficiency for MC simulation* (a small contribution of double counted events is subtracted), fraction of events in the narrow Gaussian, width of the narrow Gaussian, additional width contribution for the wide Gaussian, and the mass difference with respect to $M^{\rm PDG}_{D_{s1}} = (2535.35 \pm 0.34 \pm 0.5)$ MeV/c^2.

	$D^+\pi^-K^+$		$D^{*+}K^0$	
	data	MC	data	MC
Yield/*Efficiency*	**1264 ± 66**	*0.2699 ± 0.0017*	**5485 ± 81**	*0.1273 ± 0.0004*
Narrow Gaussian fraction	**0.59 ± 0.06**	0.463 ± 0.014	**0.63 ± 0.03**	0.629 ± 0.006
σ_1 (MeV/c^2)	**0.76 ± 0.06**	0.94 ± 0.02	**1.01 ± 0.03**	0.946 ± 0.008
$\Delta\sigma$ (MeV/c^2)	**2.4 ± 0.4**	2.55 ± 0.04	**2.54 ± 0.13**	2.56 ± 0.03
$M_{D_{s1}} - M^{\rm PDG}_{D_{s1}}$ (MeV/c^2)	**−0.57 ± 0.04**	−0.031 ± 0.010	**−0.43 ± 0.02**	−0.034 ± 0.005
Sum of intermediate branching fractions	10.53%		3.169%	

TABLE II. Systematic uncertainties for $\mathcal{B}(D_{s1}(2536)^+ \to D^+\pi^-K^+)/\mathcal{B}(D_{s1}(2536)^+ \to D^{*+}K^0)$.

Source	Uncertainty, %
Reconstruction efficiencies of low momentum $\pi^\pm$, K^+, and K^0_S from D^{*+} and $D_{s1}(2536)^+$	7.5
Particle identification of K^+ from $D_{s1}(2536)^+$	1.2
Ratio of D^+ and D^0 efficiencies	2.7
Background model in $M(D^+\pi^-K^+)$ spectrum	6.5
Efficiency dependence on $D^+\pi^-$, $K^+\pi^-$ masses and angular distribution of decay products in $D^+\pi^-K^+$ decay	1.2
Branching fraction of intermediate resonances [4]	4.1
Total	11.2

efficiency of different tracks (including pions from K^0_S) is correlated. The uncertainty in the kaon particle identification is estimated using D^{*+} decays. Uncertainty in the ratio of the remaining reconstruction efficiencies of considered final states, that is the ratio of the total D^+ and D^0 reconstruction efficiencies, is conservatively estimated by a comparison of different decay modes used in the reconstruction. One of the largest contributions to the systematic uncertainty arises due to the model of the background. It is evaluated by fitting the wrong sign $D^+\pi^+K^-$ subtracted spectrum, which contains almost no background. For the $D^+\pi^-K^+$ mode, the efficiency is almost independent of the $D^+\pi^-$, $K^+\pi^-$ masses and the angular distribution of decay products. Therefore, the possible difference between the simplified phase space MC model and the real $D_{s1}(2536)^+ \to D^+\pi^-K^+$ decay results in a small uncertainty in the efficiency determination. It is estimated by comparing the yields of events using either an average or differential efficiency in the $D_{s1}(2536)^+$ decay angles and the $D^+\pi^-$ and $K^+\pi^-$ masses. The total systematic error is found to be 11.2% (Table II).

To cross-check the results, the D^+ mass spectrum is plotted in Fig. 2 for the $D_{s1}(2536)^+$ signal and sidebands. The latter is normalized to the area of the signal interval. The sideband subtracted plot shown in the bottom of Fig. 2 is fit to a double Gaussian as above and a constant background. The resulting yield 1249 ± 66 is consistent with the yield 1262 ± 65 obtained from the fit of the $D_{s1}(2536)^+$ mass spectrum. The constant background level is found to be -0.9 ± 0.8, which is consistent with zero. The enhancement in the D^+ mass region observed in the $D_{s1}(2536)^+$ sidebands (top plot of Fig. 2) is due to combinations of a real D^+ with a random π^-K^+ pair in the event.

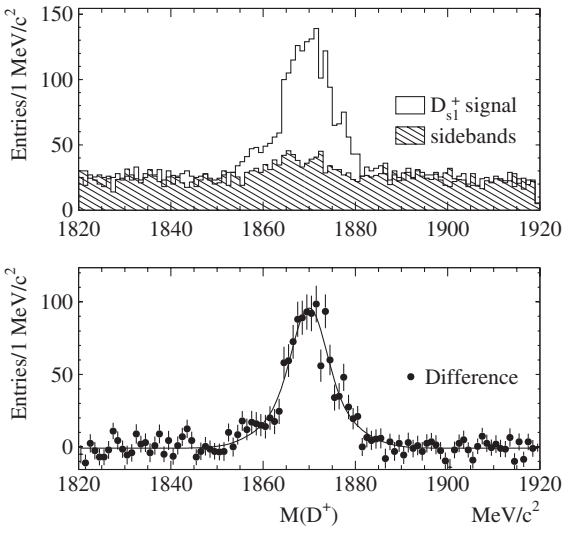

FIG. 2. D^+ mass spectrum for the $D_{s1}(2536)^+$ signal band ($|\Delta M_{D^+\pi^-K^+}| < 5$ MeV/c^2, open histogram in the top plot) and the sidebands ($10 < |\Delta M_{D^+\pi^-K^+}| < 20$ MeV/c^2, normalized to the signal interval, hatched histogram). $\Delta M_{D^+\pi^-K^+}$ is measured relative to the peak position in the top plot of Fig. 1. The bottom plot shows the sideband subtracted distribution. The solid curve shows the results of the fit described in the text.

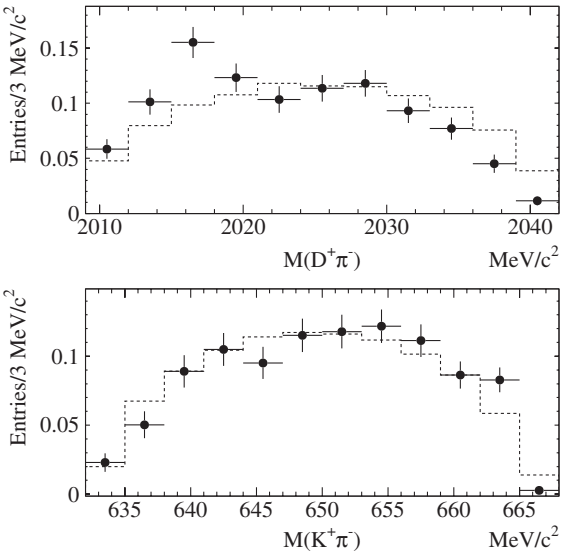

FIG. 3. Normalized mass spectra of $D^+\pi^-$ (top) and $K^+\pi^-$ (bottom) pairs from $D_{s1}(2536)^+ \to D^+\pi^-K^+$ decay obtained from fits to the $D^+\pi^-K^+$ mass distributions in different $D^+\pi^-$ or $K^+\pi^-$ mass bins. The dashed histograms show the corresponding MC distributions for $D_{s1}(2536)^+ \to D^+\pi^-K^+$ decays simulated according to a phase space distribution.

The $D^+\pi^-$ and $K^+\pi^-$ mass distributions for the $D_{s1}(2536)^+ \to D^+\pi^-K^+$ decay are shown in Fig. 3. The $D_{s1}(2536)^+$ signal yield is obtained from fits to the $D^+\pi^-K^+$ mass distribution in bins of $D^+\pi^-$ and $K^+\pi^-$ mass. All Gaussian parameters except the total number of events are fixed in the fit to the values listed in Table I. The position of the threshold used for the background description depends on the chosen bin. The areas under the histograms have been normalized to unity. The spectra are not efficiency corrected. The dashed histograms show the corresponding MC spectra for $D_{s1}(2536)^+ \to D^+\pi^-K^+$ decays simulated according to a phase space distribution. From this plot, the data points do not appear to be entirely consistent with a phase space distribution. The underlying reasons for this difference, like possible contributions from various two-body reactions (virtual D^{*0} and K^+, $D_0^*(2400)^0K^+$, $D_2^*(2460)^0K^+$, D^+ and virtual K^{*0} or higher K^* resonance), are not studied further, but the effect is taken into account in the evaluation of the systematic error on the efficiency as described above.

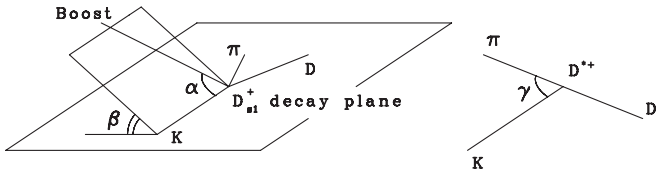

FIG. 4. Definitions of the angles α, β, and γ. The first two are measured in the $D_{s1}(2536)^+$ rest frame, the third in the D^{*+} frame. "Boost" refers to the direction of the e^+e^- center of mass in the $D_{s1}(2536)^+$ rest frame.

IV. ANGULAR ANALYSIS OF $D_{s1}(2536)^+ \to D^{*+}K_S^0$ DECAY

The $D_{s1}(2536)^+ \to D^{*+}K_S^0$ decay kinematics can be described by three angles α, β, and γ defined as shown in Fig. 4. The angles α and β are measured in the $D_{s1}(2536)^+$ rest frame: α is the angle between the boost direction of the e^+e^- center of mass and the K_S^0 momentum, while β is the angle between the plane formed by these two vectors and the $D_{s1}(2536)^+$ decay plane. The third angle γ is defined in the D^{*+} rest frame between π^+ and K_S^0.

$D_{s1}(2536)^+$ polarization can be described in terms of its helicity density matrix $\rho_{m_1m_2}$, where the indexes m_1 and m_2 denote the $D_{s1}(2536)^+$ helicities. The contribution of the element $\rho_{m_1m_2}$ to the decay amplitude is proportional to $e^{-i\phi(m_1-m_2)}$, where ϕ is the azimuthal rotation angle around the e^+e^- boost direction in the $D_{s1}(2536)^+$ rest frame. After integration over ϕ the contribution of off-diagonal elements vanishes. Because of parity conservation, the three diagonal elements can be expressed in terms of the longitudinal polarization ρ_{00}, i.e., the probability that the $D_{s1}(2536)^+$ helicity is zero. The other two probabilities are both equal to $\rho_{11} = \rho_{-1-1} = (1-\rho_{00})/2$. In the helicity formalism, the angular distribution in the decay chain $D_{s1}(2536)^+ \to D^{*+}K_S^0$, $D^{*+} \to D^0\pi^+$ is given by

$$\frac{d^3N}{d(\cos\alpha)d\beta d(\cos\gamma)} = \frac{9}{4\pi(1+2R_\Lambda)} \times \left(\cos^2\gamma\left[\rho_{00}\cos^2\alpha + \frac{1-\rho_{00}}{2}\sin^2\alpha\right] + R_\Lambda\sin^2\gamma\left[\frac{1-\rho_{00}}{2}\sin^2\beta + \cos^2\beta\left(\rho_{00}\sin^2\alpha + \frac{1-\rho_{00}}{2}\cos^2\alpha\right)\right] + \frac{\sqrt{R_\Lambda}(1-3\rho_{00})}{4}\sin2\alpha\sin2\gamma\cos\beta\cos\xi\right). \quad (3)$$

The formula depends on three variables: ρ_{00}, R_Λ, and ξ. Here $\sqrt{R_\Lambda}e^{i\xi} = A_{1,0}/A_{0,0} = z$, where $A_{1,0}$ and $A_{0,0}$ are the helicity amplitudes corresponding to the D^{*+} helicities ±1 and 0, respectively. They are related to S- and D-wave amplitudes in $D_{s1}(2536)^+$ decay by $A_{1,0} = \frac{1}{\sqrt{3}}(S + \frac{1}{\sqrt{2}}D)$, $A_{0,0} = \frac{1}{\sqrt{3}}(S - \sqrt{2}D)$. Equation (3) allows one to extract ρ_{00} and z from the $D_{s1}(2536)^+$ angular distributions and to obtain $D/S = \sqrt{2}(z-1)/(1+2z) = \sqrt{\Gamma_D/\Gamma_S}e^{i\eta}$, where $\Gamma_{D,S}$ are the partial widths of $D_{s1}(2536)^+$ and η is the phase between D- and S-amplitudes.

The interference term in Eq. (3), with phase ξ, vanishes after integration over any angle. In particular, it does not

appear in Ref. [9] in the formulas for the two- and one-dimensional distributions $d^2N/d(\cos\alpha)d(\cos\gamma)$ and $dN/d(\cos\gamma)$. Therefore, in Refs. [9,10], only $\sqrt{R_\Lambda} = |z|$ is measured for the $D_1(2420)$ meson. This only constrains the possible ranges of Γ_D/Γ_S and the phase η. To determine them unambiguously, one needs to measure the phase ξ and to fit the whole three-dimensional $d^3N/d(\cos\alpha)d\beta d(\cos\gamma)$ distribution.

The probability density function (PDF) for the unbinned maximum likelihood fit has the form

$$\mathcal{P}(\cos\alpha, \beta, \cos\gamma) = (1 - f_b) \cdot \frac{d^3N}{d(\cos\alpha)d\beta d(\cos\gamma)} \cdot \frac{\epsilon(\cos\alpha, \beta, \cos\gamma)}{\langle\epsilon\rangle_{\rm avr}} + f_b \cdot \mathcal{P}_{bck}(\cos\alpha, \beta, \cos\gamma). \quad (4)$$

It includes the efficiency corrections $\epsilon(\cos\alpha, \beta, \cos\gamma)$ and the contribution of the background $\mathcal{P}_{bck}(\cos\alpha, \beta, \cos\gamma)$. The background fraction $f_b = 528/6169$ is estimated as the ratio of the number of entries in the sidebands and in the signal region, respectively. The signal and the sideband regions, defined as $|\Delta M_{D^+_{s1}}| < 7\,\mathrm{MeV}/c^2$ and $10\,\mathrm{MeV}/c^2 < |\Delta M_{D^+_{s1}}| < 17\,\mathrm{MeV}/c^2$, respectively, are wider than in the $D^+\pi^-K^+$ case since the background is lower. The PDF $\mathcal{P}_{bck}(\cos\alpha, \beta, \cos\gamma)$, which is normalized to unity, is modeled using the sideband event distribution and the procedure described below. $\epsilon(\cos\alpha, \beta, \cos\gamma)$ is the MC-determined efficiency. The average efficiency $\langle\epsilon\rangle_{\rm avr}$ normalizes to unity the signal part of the PDF. It is recalculated in every iteration of the fit procedure as $\langle\epsilon\rangle_{\rm avr} \equiv \sum_i \epsilon_i \cdot I_i \approx \iiint \frac{d^3N}{d(\cos\alpha)d\beta d(\cos\gamma)} \times \epsilon(\cos\alpha, \beta, \cos\gamma)d(\cos\alpha)d\beta d(\cos\gamma)$. The sum is taken over $10 \times 10 \times 10$ "bins" in a three-dimensional $(\cos\alpha) \times \beta \times (\cos\gamma)$ space. The efficiency map ϵ_i is determined from MC simulation, while the integral I_i of $d^3N/d(\cos\alpha)d\beta d(\cos\gamma)$ over each bin volume is calculated analytically.

The density $\mathcal{P}_{bck}(\cos\alpha, \beta, \cos\gamma)$ of sideband events in the vicinity of $(\cos\alpha, \beta, \cos\gamma)$ is calculated as follows. First, the three-dimensional $(\cos\alpha) \times \beta \times (\cos\gamma)$ space is rescaled along each axis to the unit cube. This ensures that in the case of uniform distributions all three variables have the same "weight." Then, for the given point $(\cos\alpha, \beta, \cos\gamma)$, we find the volume V_{10} (V_{11}) of the smallest cube centered at this point and containing 10 (11) the closest sideband events. The 10th (11th) event lies on a surface of V_{10} (V_{11}). Therefore, we assign 10 full events to the volume $V_{10.5} \equiv \frac{1}{2}(V_{10} + V_{11})$ and estimate $\mathcal{P}_{bck}(\cos\alpha, \beta, \cos\gamma) = 10/V_{10.5}/(4\pi \cdot 528)$. Here, 4π is the original volume of the $(\cos\alpha) \times \beta \times (\cos\gamma)$ space and 528 is the total number of sideband events. The resulting $\mathcal{P}_{bck}$ is thus normalized. To determine a systematic uncertainty due to this procedure, we estimate the background density $\mathcal{P}_{bck}$ using 20 or 50 closest sideband events instead of 10. The changes are found to be negligible compared to statistical errors (see below).

The advantage of this procedure is that for any one signal event $\mathcal{P}_{bck}$ is always determined from 10 (or 20, or 50) sideband events. Therefore the sideband fluctuations are much smaller than fluctuations of one signal event. This ensures the necessary degree of "smoothness" of the $\mathcal{P}_{bck}$ distribution. On the other hand, the typical volume $V_{10.5}$ is about $10/528 \approx 0.02$ of the whole $(\cos\alpha) \times \beta \times (\cos\gamma)$ space volume. $\mathcal{P}_{bck}$ thus reproduces the background behavior at this level of granularity.

A similar method is used to construct the efficiency function $\epsilon(\cos\alpha, \beta, \cos\gamma)$. Because of the much larger MC sample, instead of $V_{10.5}$ we use the volume with 100 MC reconstructed events $V_{100.5}$. We then determine the number of MC events generated there, $N^{100}_{\rm gen}$, and calculate the efficiency as $\epsilon(\cos\alpha, \beta, \cos\gamma) = 100/N^{100}_{\rm gen}$. As in the previous case, usage of the 50 or 200 closest events instead of 100 reproduces the same results within the statistical errors, and is used to determine the systematic uncertainty of this method due to the efficiency.

The three-dimensional fit of all $D_{s1}(2536)^+$ signal entries to $\mathcal{P}(\cos\alpha, \beta, \cos\gamma)$ gives

$$z = A_{1,0}/A_{0,0} = \sqrt{R_\Lambda}e^{i\xi} = \sqrt{3.6 \pm 0.3 \pm 0.1}\exp(\pm i \cdot (1.27 \pm 0.15 \pm 0.05)). \quad (5)$$

Note that the angular distributions are sensitive only to $\cos\xi$, not to ξ itself. Therefore ξ has a $\pm\xi + 2\pi n$ ambiguity, and $A_{1,0}/A_{0,0}$ is determined up to complex conjugation. The average $D_{s1}(2536)^+$ longitudinal polarization in the region $x_P > 0.8$ is measured to be $\rho_{00} = 0.490 \pm 0.012 \pm 0.004$.

Systematic uncertainties are calculated as a sum in quadrature of the contributions listed in Table III. MC simulation shows that the detector resolution in $\cos\alpha$, β, $\cos\gamma$ not only increases the final errors but also effectively decreases the parameter R_Λ by 0.13. The corresponding correction has already been applied to the above result. The systematic uncertainties in modelling $\mathcal{P}_{bck}$ and ϵ are estimated by varying the number of closest sideband or simulated events as explained above, and by using different sidebands: $7\ \mathrm{MeV}/c^2 < |\Delta M_{D_{s1}(2536)^+}| < 10\ \mathrm{MeV}/c^2$ plus $17\ \mathrm{MeV}/c^2 < |\Delta M_{D_{s1}(2536)^+}| < 21\ \mathrm{MeV}/c^2$ (instead

TABLE III. Systematic uncertainties for R_Λ, ξ, and ρ_{00}.

Source	R_Λ	ξ	ρ_{00}
Angular resolution	0.05	0.02	0.001
Modeling of $\mathcal{P}_{bck}$ and efficiency	0.04	0.00	0.001
Different sidebands	0.03	0.02	0.002
MC statistics	0.07	0.04	0.003
Total	0.10	0.05	0.004

of $10\ \mathrm{MeV}/c^2 < |\Delta M_{D_{s1}(2536)^+}| < 17\ \mathrm{MeV}/c^2$). The errors due to statistical fluctuation of the MC sample, which is 15.4 times larger than data and has almost the same R_Λ, ξ, and ρ_{00}, are calculated as $\sqrt{1/15.4} = 0.25$ of the statistical errors.

The ratio of D- and S-wave amplitudes is found to be $D/S = (0.63 \pm 0.07 \pm 0.02) \cdot \exp(\pm i \cdot (0.76 \pm 0.03 \pm 0.01))$. The relative phase is close to $\pi/4$, $(43.8 \pm 1.7 \pm 0.6)^\circ$. One can see that, contrary to the HQET prediction, the S-wave dominates. Its contribution to the total width is $1/(1 + |D/S|^2) = \Gamma_S/\Gamma_{\mathrm{total}} = 0.72 \pm 0.05 \pm 0.01$.

The background-subtracted efficiency corrected and normalized one-dimensional projections of $d^3N/d(\cos\alpha)d\beta d(\cos\gamma)$ distribution, together with the fit results, are shown in Fig. 5. The χ^2 difference between the points and the projected fit results corresponds to a goodness-of-fit probability of about 60%. As mentioned earlier, one-dimensional projections are not sensitive to the phase ξ. They are described instead by the following formulas derived from Eq. (3):

$$\frac{dN}{d\cos\alpha} = \frac{3}{4(1+2R_\Lambda)}\{[(1+R_\Lambda) + (R_\Lambda - 1)\rho_{00}] + \cos^2\alpha(R_\Lambda - 1)(1 - 3\rho_{00})\}, \quad (6)$$

$$\frac{dN}{d\beta} = \frac{1}{\pi(1+2R_\Lambda)}\{[1 + 3R_\Lambda(1-\rho_{00})] + 2R_\Lambda(3\rho_{00} - 1)\cos^2\beta\}, \quad (7)$$

$$\frac{dN}{d\cos\gamma} = \frac{3}{2(1+2R_\Lambda)}\{\cos^2\gamma + R_\Lambda \sin^2\gamma\}. \quad (8)$$

In spite of the complexity of Eq. (3), it depends only quadratically on $\sqrt{R_\Lambda}$ and only linearly on $\cos\xi$ and ρ_{00}. The efficiency entering the PDF in Eq. (4) is almost constant in all three projections. When it is set to a constant value in the fit, the results change by less than 1/3 of the statistical error. The background fraction $f_b = 9\%$ is small. Therefore one does not expect any significant biases of the fit results.

To quantify this statement, 1000 samples of events are generated according to PDF Eq. (4). Each sample contains the same number of events as observed in data. The parameters R_Λ, ξ, and ρ_{00} are set to the values determined from data. A three-dimensional fit is performed for each sample; it is verified that the fit results are not systematically biased and the errors are estimated correctly. The value of the overall likelihood function is measured to be worse than the one observed in data in 33% of cases.

As a final check, the fit to data is repeated in different bins of the mass recoiling against the $D_{s1}(2536)^+$, defined as $\sqrt{(2E^*_{\mathrm{beam}} - E^*_{D^+_{s1}})^2 - (p^*_{D^+_{s1}})^2}$, where all quantities are measured in the e^+e^- center-of-mass frame. The parameters R_Λ and ξ are found to be independent of $D_{s1}(2536)^+$ momentum or recoil mass within statistical errors. The recoil mass spectrum is shown in the top half of Fig. 6. The resolution is about 70 MeV/c^2 at 2 GeV/c^2 and is approximately inversely proportional to the recoil mass. There is an indication of two-body contributions from $e^+e^- \to D_{s1}(2536)^+X$ where $X = D_s^+$, D_s^{*+}, and higher D_s^{**+} resonances. This agrees with the $D_{s1}(2536)^+$ polarization spectrum, shown in the bottom half of Fig. 6, which also exhibits some structure at low recoil masses. This spectrum is obtained when R_Λ and ξ are fixed to their values determined from the overall fit. At D_s^+ mass, as one expects, the longitudinal polarization is low. It then rises rapidly at the D_s^{*+} mass and eventually reaches a plateau at $\rho_{00} \approx 0.5$.

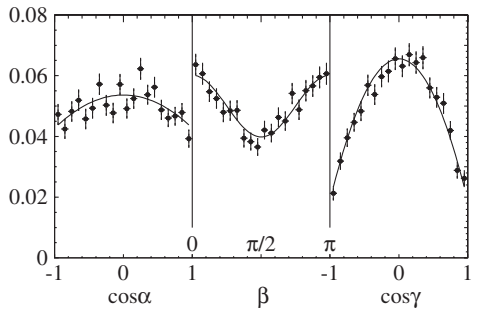

FIG. 5. Background subtracted, efficiency corrected, and normalized one-dimensional $\cos\alpha$, β, $\cos\gamma$ angular distributions. Projected results of the three-dimensional fit are shown by the solid curves.

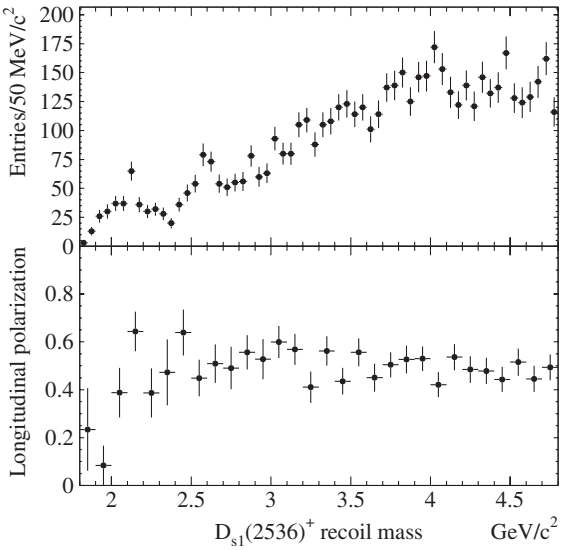

FIG. 6. $D_{s1}(2536)^+$ recoil mass spectrum (top), probability ρ_{00} that $D_{s1}(2536)^+$ helicity is zero (bottom). The decrease at low values in the bottom plot can be attributed to the contribution of two-body $e^+e^- \to D_{s1}(2536)^+X$ reactions.

V. CONCLUSIONS

In conclusion, a new decay channel $D_{s1}(2536)^+ \to D^+\pi^-K^+$ is observed. The $D^+\pi^-$ pair is the only $D\pi$ combination that cannot come from a D^* resonance. It can be produced only through the virtual D^{*0}, broad $D_0^*(2400)^0$, or $D_2^*(2460)^0$ resonances. In addition, the $D^+\pi^-K^+$ final state can be formed by two-body decays to a D^+ and a virtual K^{*0} or higher K^* resonance. No clear resonant substructure is found in the $D^+\pi^-K^+$ system. The ratio of branching fractions $\mathcal{B}(D_{s1}(2536)^+ \to D^+\pi^-K^+)/\mathcal{B}(D_{s1}(2536)^+ \to D^{*+}K^0)$ is measured to be $(3.27 \pm 0.18 \pm 0.37)\%$.

An angular analysis of the decay $D_{s1}(2536)^+ \to D^{*+}K_S^0$ is also performed. Since the c-quark is not infinitely heavy, HQET is violated and the $D_{s1}(2536)^+$ can contain an admixture of another $J^P = 1^+$ state with $j = 1/2$ and can decay in an S-wave. The energy release in this reaction is small. Therefore the D-wave is suppressed by the barrier factor $(q/q_0)^5$, where q is the relative momentum of $D_{s1}(2536)^+$ decay products in the $D_{s1}(2536)^+$ rest frame, and q_0 is a momentum scale characteristic of the decay. The S-wave contribution to the total width is proportional to q/q_0 and can be sizeable even if the mixing is small. Using an unbinned maximum likelihood fit to the three angles in the $D_{s1}(2536)^+ \to D^{*+}K_S^0$, $D^{*+} \to D^0\pi^+$ decay chain, we measure (up to a complex conjugation) the ratio of S- and D-wave amplitudes: $D/S = (0.63 \pm 0.07 \pm 0.02) \cdot \exp(\pm i \cdot (0.76 \pm 0.03 \pm 0.01))$. The S-wave dominates, and its contribution to the total width is $\Gamma_S/\Gamma_{\text{total}} = 0.72 \pm 0.05 \pm 0.01$. This result allows to calculate the mixing angle in the theoretical models with a known value of parameter q_0 [8,12].

The spin of high momentum $D_{s1}(2536)^+$ mesons produced in e^+e^- annihilation prefers to align transversely to the momentum. The probability that a $D_{s1}(2536)^+$ with $x_P > 0.8$ has zero helicity is found to be $\rho_{00} = 0.490 \pm 0.012 \pm 0.004$. Assuming the HQET relation $\rho_{00} = \frac{2}{3} \times (1 - w_{3/2})$ [13], this implies a value of the Falk-Peskin parameter, $w_{3/2} = 0.266 \pm 0.018 \pm 0.006$, in this momentum region. This value is close to the prediction of Ref. [17], $w_{3/2} \approx 0.254$, obtained for the entire momentum region, although the applicability of the perturbative QCD fragmentation model for D_s^{**+} mesons is questionable.

ACKNOWLEDGMENTS

We thank the KEKB group for the excellent operation of the accelerator, the KEK cryogenics group for the efficient operation of the solenoid, and the KEK computer group and the National Institute of Informatics for valuable computing and Super-SINET network support. We acknowledge support from the Ministry of Education, Culture, Sports, Science, and Technology of Japan and the Japan Society for the Promotion of Science; the Australian Research Council and the Australian Department of Education, Science and Training; the National Science Foundation of China and the Knowledge Innovation Program of the Chinese Academy of Sciences under Contract No. 10575109 and No. IHEP-U-503; the Department of Science and Technology of India; the BK21 program of the Ministry of Education of Korea, the CHEP SRC program and Basic Research program (Grant No. R01-2005-000-10089-0) of the Korea Science and Engineering Foundation, and the Pure Basic Research Group program of the Korea Research Foundation; the Polish State Committee for Scientific Research; the Ministry of Education and Science of the Russian Federation and the Russian Federal Agency for Atomic Energy; the Slovenian Research Agency; the Swiss National Science Foundation; the National Science Council and the Ministry of Education of Taiwan; and the U.S. Department of Energy.

[1] B. Aubert *et al.* (*BABAR* Collaboration), Phys. Rev. Lett. **90**, 242001 (2003); D. Besson *et al.* (CLEO Collaboration), Phys. Rev. D **68**, 032002 (2003); A. Drutskoy *et al.* (Belle Collaboration), Phys. Rev. Lett. **94**, 061802 (2005).
[2] P. Krokovny *et al.* (Belle Collaboration), Phys. Rev. Lett. **91**, 262002 (2003).
[3] Y. Mikami *et al.* (Belle Collaboration), Phys. Rev. Lett. **92**, 012002 (2004).
[4] W.-M. Yao *et al.* (Particle Data Group), J. Phys. G **33**, 1 (2006).
[5] See P. Colangelo, F. De Fazio, and R. Ferrandes, Mod. Phys. Lett. A **19**, 2083 (2004); E. S. Swanson, Phys. Rep. **429**, 243 (2006), and references therein.
[6] B. Aubert *et al.* (*BABAR* Collaboration), Phys. Rev. D **74**, 032007 (2006).
[7] N. Isgur and M. Wise, Phys. Rev. Lett. **66**, 1130 (1991); M. Lu, M. Wise, and N. Isgur, Phys. Rev. D **45**, 1553 (1992).
[8] S. Godfrey, Phys. Rev. D **72**, 054029 (2005).
[9] P. Avery *et al.* (CLEO Collaboration), Phys. Lett. B **331**, 236 (1994); **342**, 453(E) (1995).
[10] T. Bergfeld *et al.* (CLEO Collaboration), Phys. Lett. B **340**, 194 (1994).
[11] Y. Yamada *et al.*, Phys. Rev. C **72**, 065202 (2005).
[12] S. Godfrey and R. Kokoski, Phys. Rev. D **43**, 1679 (1991); N. Isgur, Phys. Rev. D **57**, 4041 (1998); W. Lucha and F. F. Schöberl, Mod. Phys. Lett. A **18**, 2837 (2003).
[13] A. Falk and M. Peskin, Phys. Rev. D **49**, 3320 (1994).
[14] Y. Kubota *et al.* (CLEO Collaboration), Phys. Rev. D **44**,

593 (1991); G. Brandenburg *et al.* (CLEO Collaboration), Phys. Rev. D **58**, 052003 (1998).
[15] S. Abachi *et al.* (HRS Collaboration), Phys. Lett. B **199**, 585 (1987); S. Aihara *et al.* (TPC Collaboration), Phys. Rev. D **43**, 29 (1991); K. Ackerstaff *et al.* (OPAL Collaboration), Z. Phys. C **74**, 437 (1997); K. Abe *et al.* (SLD Collaboration), The International Symposium on Lepton and Photon Interactions (LP97), Hamburg, Germany, 1997, Report No. SLAC-PUB 7574.
[16] A. David, Phys. Lett. B **644**, 224 (2007).
[17] T. C. Yuan, Phys. Rev. D **51**, 4830 (1995); Y.-Q. Chen and M. Wise, Phys. Rev. D **50**, 4706 (1994); Y.-Q. Chen, Phys. Rev. D **48**, 5181 (1993).
[18] H. Albrecht *et al.* (ARGUS Collaboration), Phys. Lett. B **221**, 422 (1989).
[19] S. Kurokawa and E. Kikutani, Nucl. Instrum. Methods Phys. Res., Sect. A **499**, 1 (2003) and other papers included in this volume.
[20] A. Abashian *et al.* (Belle Collaboration), Nucl. Instrum. Methods Phys. Res., Sect. A **479**, 117 (2002).
[21] Z. Natkaniec *et al.* (Belle SVD2 Group), Nucl. Instrum. Methods Phys. Res., Sect. A **560**, 1 (2006).
[22] E. Nakano, Nucl. Instrum. Methods Phys. Res., Sect. A **494**, 402 (2002).
[23] EvtGen home p. http://www.slac.stanford.edu/~lange/EvtGen; see also D. Lange, Nucl. Instrum. Methods Phys. Res., Sect. A **462**, 152 (2001).
[24] T. Sjöstrand *et al.* (PYTHIA Collaboration), Comput. Phys. Commun. **135**, 238 (2001).
[25] R. Brun *et al.* (GEANT Collaboration), GEANT Report No. 3.21, CERN Report No. DD/EE/84-1, 1984.
[26] We use two iterations, generating first a pure D-wave $D_{s1}(2536)^+ \to D^{*+}K^0_S$ decay with $D_{s1}(2536)^+$ polarization and momentum predicted by PYTHIA, and in the second step according to the results obtained using the first MC sample. After two iterations the values used to generate the MC sample and the results differ by a negligible amount.